



# Recent applications of phthalocyanines and naphthalocyanines for imaging and therapy

Yumiao Zhang<sup>1,2</sup> and Jonathan F. Lovell<sup>1\*</sup>

With high extinction coefficients and long absorption wavelengths in the near infrared region, phthalocyanines (Pcs) and naphthalocyanines (Ncs) are well-suited for optical imaging and phototherapies in biological tissues. Pcs and Ncs have been used in a range of theranostic applications. Peripheral and axial substituents can be introduced to Pcs and Ncs for chemical modification. Seamless metal chelation of Pcs or Ncs can expand their possibilities as medical therapeutic and imaging agents. Nanoparticulate approaches enable unique ways to deliver Pcs and Ncs to target tissues and improve their solubility, biocompatibility, biodistribution and stability. Herein, we highlight some recent Pc or Nc nanoscale systems for theranostic applications. © 2016 Wiley Periodicals, Inc.

How to cite this article:

*WIREs Nanomed Nanobiotechnol* 2016. doi: 10.1002/wnan.1420

## INTRODUCTION

Compared to the related tetrapyrrolic porphyrins and chlorins, phthalocyanines (Pcs) and naphthalocyanines (Ncs) generally exhibit longer absorption wavelengths and higher extinction coefficients (typically on the order of  $10^5/\text{M}/\text{cm}$ ) in the near infrared (NIR) region.<sup>1</sup> Pcs have an additional benzene ring fused to each of the four pyrrolic subunits (Figure 1(a) and (b)) which causes more electron delocalization and increases absorption at longer wavelengths. The four pyrroles comprise a macrocycle well suited to form coordination complexes with a variety of metals chelated in the center. Pcs have been widely used in the areas of laser printer, recordable compact disks, nonlinear optical materials, industrial catalysts, and photosensitizers in phototherapy.<sup>2–5</sup> Ncs have two additional

cyclohexadiene rings on each pyrrole group (Figure 1(c)). Ncs generally absorb even longer wavelengths than Pcs, making them, in theory, well suited for optical applications in deep tissue biological tissues. However, with proper quantum design Pcs also can have long wavelength absorption peaks beyond 1000 nm.<sup>6</sup> Like Pcs, it is also feasible to chelate metals in the center of Ncs. Nc-based dyes have been used as photosensitizers in energy harvesting studies.<sup>7</sup> Upon illumination, photosensitizers are excited by a photon transition between the ground state and a singlet excited state, and can ultimately culminate with conversion of oxygen to reactive oxygen species (ROS) as shown in Figure 1(d). In the ground state ( $S_0$ ), electrons are in the lowest energy orbitals. Upon absorption of light with appropriate energy, electrons in photosensitizers are shifted to an excited singlet state and that is sectioned in different vibrational levels with increasing energy. Electrons fall from higher vibrational level to the lowest energy level of that excited state via vibrational relaxation. From the excited state, the molecule tends to return back to  $S_0$  after a short period. Excited molecules can return to the ground state via photon emission or quenching that comes with the generation of heat. Heat dissipation in this way is the basis for photothermal

\*Correspondence to: jflovell@buffalo.edu

<sup>1</sup>Department of Biomedical Engineering, University at Buffalo State University of New York, Buffalo, NY, USA

<sup>2</sup>Department of Chemical and Biological Engineering, University at Buffalo State University of New York, Buffalo, NY, USA

Conflict of interest: The authors have declared no conflicts of interest for this article.

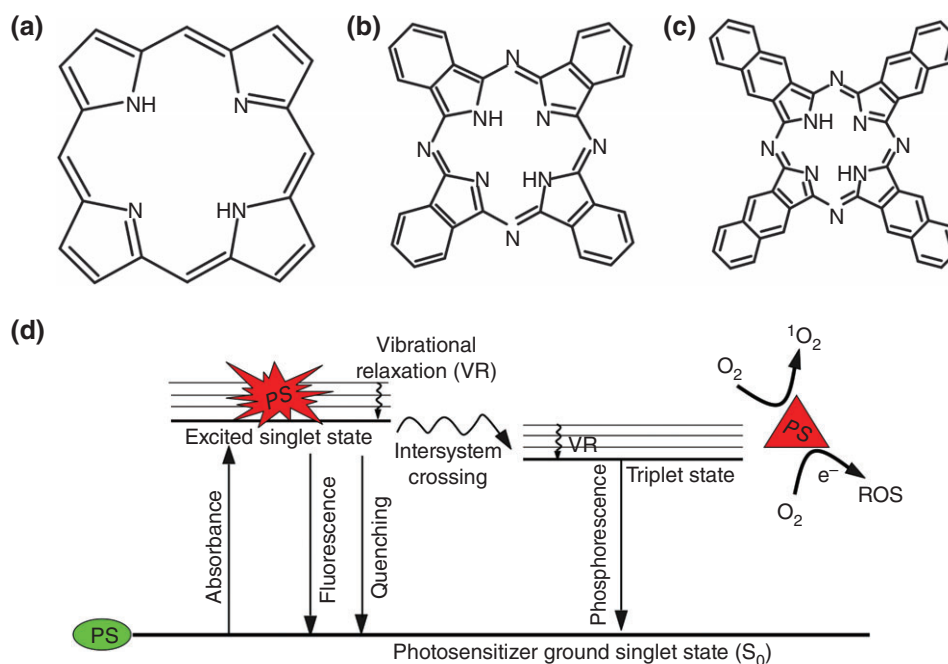


**FIGURE 1** | Chemical structure of (a) porphyrins (b) phthalocyanines, and (c) naphthalocyanines. (d) Simplified Jablonski diagram showing some possible activated singlet oxygen deactivation pathways. PS and ROS represent photosensitizers and reactive oxygen species, respectively. Green and red indicate ground and excited state photosensitizers, respectively.

therapies. If the molecule does not rapidly return to the ground state, it may move from the singlet state to triplet state via intersystem crossing, enabling phosphorescence or reactive oxygen sensitization.<sup>8</sup>

Organic dyes play a central role in biomedical imaging due to their versatile photophysical properties and availability for large-scale synthesis. Organic dyes are feasible to conjugate with various specific biomolecules for a wide variety of assays. Compared to inorganic photonic nanoparticles, small molecule dyes can be more reproducibly generated and characterized, which has advantages from a regulatory perspective. Pcs and Ncs are promising due to their long wavelength absorption of light, which enables deeper tissue penetration. However, their application has probably been limited by their poor water solubility and tendency to aggregate. Consequently, once irradiated with NIR light, the aggregated molecules dissipate heat and applications such as fluorescence imaging or ROS production can be diminished. On the other hand, aggregated and fluorescently quenched properties are not problematic for generating thermal expansion waves for photoacoustic imaging or photothermal therapy.<sup>9,10</sup> Regardless of photophysical properties, injectable Pc and Ncs require solubilization to avoid very large aggregates, which would cause adverse injection reactions.<sup>11</sup> To overcome the poor water solubility, many

solubilization strategies have been developed including using nanocarriers and chemical modifications.

Several Pc formulations have reached clinical testing.<sup>12</sup> Water soluble sulfonated AlPc (trade name: Photosens) can be directly dissolved in water and has been explored in multiple types of cancer photo treatments including skin, breast, lung oropharyngeal, larynx, neck, larynx and cervical cancers. For the treatment of carcinoma of the upper aerodigestive tract, ZnPc was encapsulated in liposomes made of POPC (palmitoyl-oleoyl-phosphatidylcholine) and DOPS (dioleoyl phosphatidylserine). A di-sulfonic-di-phthalimidomethyl ZnPc-based Cremophor EL formulation was also tested in phase I clinical trials for the treatment of skin or esophageal cancer. Silicon-based Pc formulations dissolved in propylene glycol (for topical administration) or in Cremophor EL (for intravenous administration) together with ethanol and reached clinical testing for various skin diseases and cancers. Copper Pcs can be used as blue pigment for tattoo inks; however, it has been shown that laser removal might induce toxicity due to the formation of decomposition products upon laser irradiation.<sup>13</sup> Moving forward, more testing will be useful to better understand the toxicity profile of Pcs and Ncs. In this review, we summarize emerging applications of Pcs and Ncs for theranostic use with a particular emphasis on nanosystems.

## BIOIMAGING USING Pcs and Ncs

Biomedical imaging techniques can provide important information and insight for early detection and diagnosis of diseases. Ncs and Pcs have been used as contrast agents in imaging modalities including magnetic resonance imaging (MRI), fluorescence imaging, positron emission tomography (PET), photoacoustic imaging and others. Combinations of these imaging techniques have resulted in numerous studies on higher-order, multimodalities using contrast agents with multifunctional capabilities in one single nanoparticle.<sup>14</sup> Photoacoustic tomography is an emerging optical imaging technique with high resolution based on photoacoustic effect and is useful for imaging chemicals and drugs.<sup>15,16</sup> Pcs and Ncs generally have higher extinction coefficients than those of porphyrins, hence they are expected to provide better contrast for photoacoustic imaging. Pc- and Nc-based contrast agents are also used for fluorescence imaging. Optical fluorescence imaging offers the advantages of high sensitivity, low cost and high speed but can be limited by fluorescence quenching within Pcs and Ncs. Strategies have been developed to restore the fluorescence such as hydrophilic modifications. It was shown that modified graphene nanosheets could be used to prevent the aggregation of Pc and thereby enable fluorescence imaging guidance for phototherapy.<sup>17</sup> PET has been used as a clinical imaging tool for decades. MRI and functional MRI, based on the nuclear spin and resonance radiofrequency absorption in an external magnetic field, can provide tissue-specific differences and even metabolic activities due to the different transverse and longitudinal relaxation rates for different tissues. It has been shown that tetrapyrrole structures are able to chelate a diverse range of metals including Mn, Fe, Cu, Ga, Gd, and others in the center of the macrocycle<sup>18</sup> and metal-chelated tetrapyrrole photosensitizers have been used contrast agents for PET and MRI imaging of tumors with a long history, dating back to 1952<sup>19</sup> and 1987,<sup>20</sup> respectively.

### Polymeric Nanoparticles and Micelles for Bioimaging

Polymeric nanoparticles are advantageous with respect to their chemically tunable size and modifiable surface groups, resulting in applications in controlled release and targeting. Recently, Nc-based biodegradable polymeric nanoparticles have been made for *in vivo* fluorescence imaging and photothermal therapy.<sup>21</sup> The theranostic nanoparticles consist of silicon naphthalocyanine (SiNc) as a contrast and therapeutic agent and the copolymer poly (ethylene glycol)-block-

poly caprolactone (PEG-PCL) (Figure 2(a)) as the dye carrier. Indocyanine green (ICG), a clinically used NIR dye, has also been considered for promising theranostic nanoplatfoms<sup>22,23</sup> but on the other hand, exhibits poor photostability and the fluorescence signal might disappear during imaging-guided process due to photodegradation of the dye.<sup>24</sup> It was shown that the Nc polymeric nanoparticles have superior stability under extensive light irradiation.<sup>21</sup> SiNc polymeric nanoparticles also have improved long-term colloidal stability in addition to photostability.<sup>25</sup> Silicon 2,3-naphthalocyanine bis (trihexylsilyloxy) (NIR 775) was co-encapsulated with 2,3-bis (4-(phenyl (4-(1,2,2-triphenylvinyl)phenylamino)phenyl) fumaronitrile (TPETPAFN) into the matrix of 1,2 distearoyl-sn-glycero-3-phosphoethanolamine-N-[methoxy(polyethyleneglycol)-2000] (DSPE-PEG2000, Figure 2(b)). Owing to spectral overlap of the emission of TPETPAFN and absorption of NIR 775, the fluorescent nanoparticles exhibited a 47-fold enhancement of emission intensity of NIR 775 upon excitation of TPETPAFN at 510 nm compared to direct excitation of NIR 775. This system, based on Forster resonance energy transfer (FRET), showed good photostability and low cytotoxicity. Further research demonstrated similar properties in other studies.<sup>26</sup> Silicon 2,3-naphthalocyanine bis (trihexylsilyloxy) (SiNc) dye doped in a matrix polymer poly [2-methoxy-5-(2-ethylhexyloxy)-1,4-phenylenevinylene] (MEH-PPV, Figure 2(c)) was encapsulated in amphiphilic polymer, polystyrene-graft-ethylene oxide functionalized with carboxyl groups (PS-PEG-COOH, Figure 2(d)). To avoid the self-quenching effects and to optimize the FRET efficiency, the ratio of SiNc to MEH-PPV matrix was adjusted around 1%. This FRET system also enables the excitons to migrate along the polymer chain over long distances, and such amplified FRET process was also facilitated by the large extinction coefficient of Nc dye. Furthermore, the stability during 9 months was demonstrated, providing superior fluorescence contrast with whole body animal tumor imaging. This is also in agreement with previous result showing that the fluorescence of Ncs can become quenched inside nanoparticles.<sup>27</sup> Compared to liposomes or other carriers, the long-term safety and biocompatibility are possible concerns for polymeric carriers even though they hold potential for a range of chemical modifications.

Recently, a family of Pc and Nc Pluronic micelles, termed nanonaps was developed based on the hydrophobic interactions between extremely hydrophobic Ncs and Pcs and the hydrophobic poly (propylene oxide) block of Pluronic F127 (Figure 2(e)).<sup>27</sup> At low temperatures, the free and loose

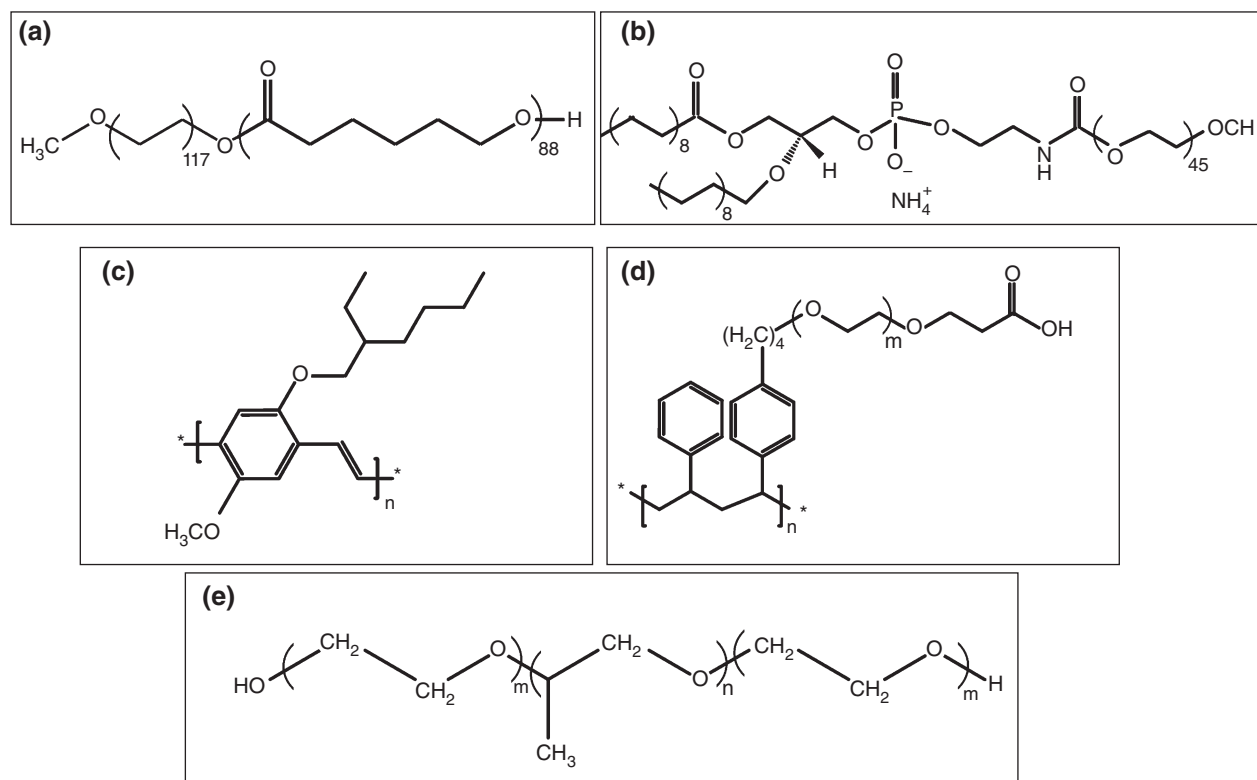


**FIGURE 2** | Chemical structures of some polymers used as Pc and Nc carriers. (a) Poly (ethylene glycol)-block-poly caprolactone (PEG-PCL). (b) 1,2 distearoyl-*sn*-glycero-3-phosphoethanolamine-*N*-[methoxy(polyethylene glycol)-2000]. (DSPE-PEG<sub>2000</sub>). (c) Poly [2-methoxy-5-(2-ethylhexyloxy)-1,4-phenylenevinylene] (MEH-PPV). (d) Carboxyl polystyrene-graft-ethylene oxide, PS-PEG-COOH. (e) Pluronic block copolymer,  $m = 100$ ,  $n = 65$  for Pluronic F127.

surfactant could be stripped and frozen micelles were concentrated in solution with tremendously high calculated NIR absorbance values (>1000) without spectral shifting. Nanonaps were employed for intestinal contrast imaging, as they safely passed through the gastrointestinal tract without systematic absorption following oral administration. Noninvasive real-time photoacoustic images of intestine were obtained to visualize the nanonap distribution and intestine function in mice with good resolution and low background. In addition,  $^{64}\text{Cu}$  was post-labeled in the center of the Nc dye. Whole body PET imaging with high resolution can be achieved by this sensitive and clinically established imaging approach without any limitation of penetration depth (Figure 3). These nanoparticles were also used to demonstrate spectrally resolved imaging of lymphatic systems using two-color, dual channel photoacoustic imaging.<sup>28</sup>

### Liposomal Formulations for Bioimaging

Most Pcs or Ncs, characterized by the flat aromatic macrocycle, are not soluble in water and liposomes are another commonly used carrier system that has

been used to improve their solubility. Liposome cargo can exchange with serum lipoproteins following systemic administration. Because of receptor-mediated transport mechanisms that enable low-density lipoproteins to bind to tumor cells,<sup>29</sup> liposomes could facilitate targeting of photosensitizers efficiently *in vivo* even at a low dose.<sup>30</sup> Zinc phthalocyanine (ZnPc) was loaded in unilamellar liposomes by a solvent exchange method.<sup>31</sup> After intravenous injection, the fluorescence of the tumor and blood vessels increased and fluorescence of blood in circulation reached a plateau after 120 min. The increase was ascribed to the release of the dye in circulation whereas the fluorescence in tumor sites increased more slowly, which was explained by the fact that ZnPc was taken up by lipoprotein prior to accumulation by the tumor cells via an active process. However, one potential problem of Pc-based photosensitizers for fluorescence imaging during PDT monitoring is photobleaching of photosensitizers upon irradiation. Hydrophilic tetrasulfonated aluminum phthalocyanine (AlPcS<sub>4</sub>) and hydrophobic Zinc phthalocyanine (ZnPc) in liposomal form were compared in a rat tumor model.<sup>32</sup> Photobleaching of ZnPc was observed both *in vivo* and

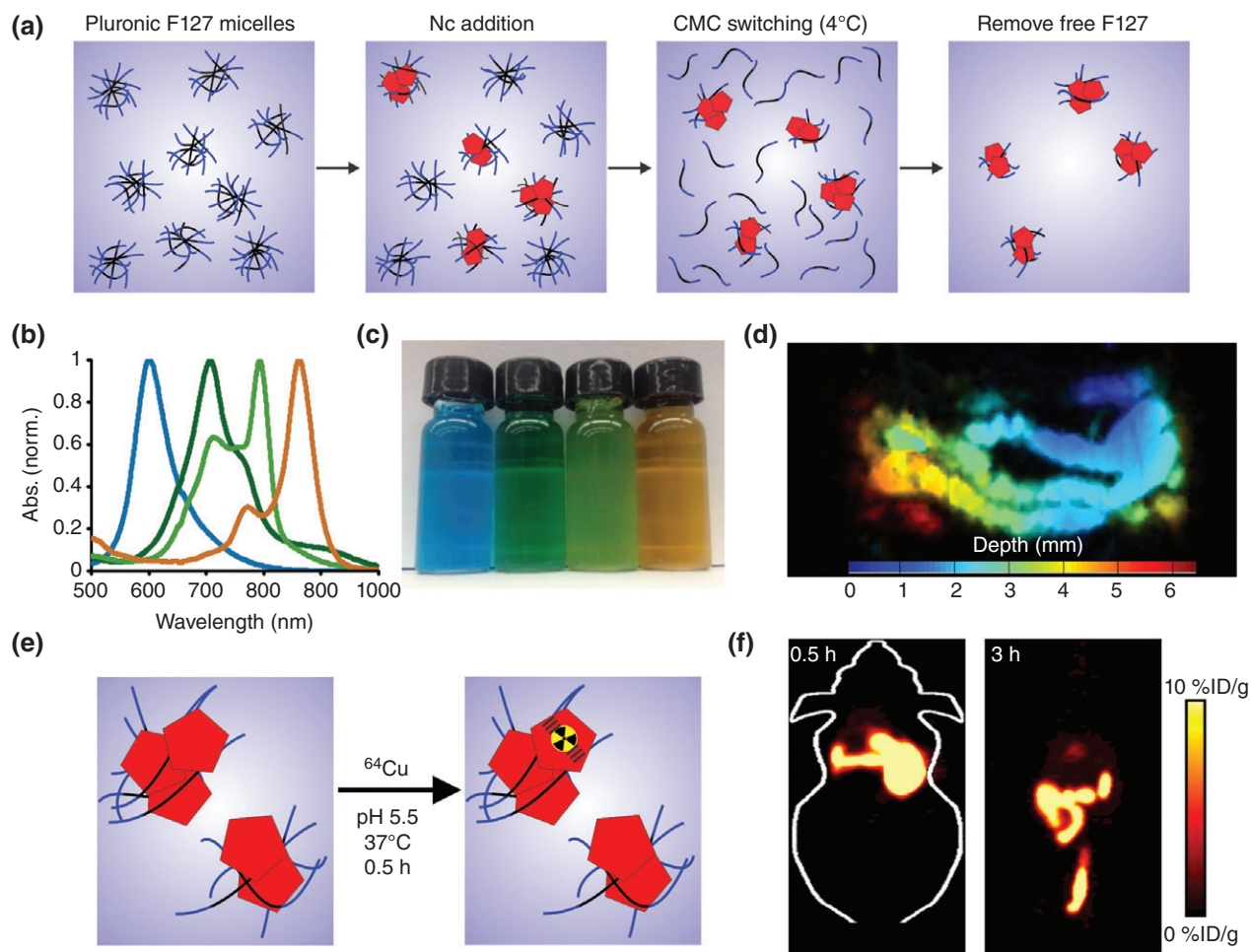


**FIGURE 3** | Noninvasive and multimodal imaging using surfactant-stripped nanoformulated naphthalocyanines (nanonaps). (a) Schematic illustration of nanonaps. PEO, PPO, Nc dyes are in blue, black and red, respectively. (b) Normalized absorbance of nanonaps formed from BPC (blue), ZnBNC (dark green), BNC (light green), or ONC (bronze). (c) Photographs of nanonaps in water, from left to right: BPC, ZnBNC, BNC, ONC. (d) Depth encoded PA MIP (maximum intensity of projection) of the intestine visualizing ZnBNC nanonaps. (e) Nanonaps labeling using  $^{64}\text{Cu}$ , Pluronic F127 PEO blocks, PPO blocks and Nc dye are in blue, black, and red, respectively and  $^{64}\text{Cu}$  is shown as the radioactive yellow circle. (f) Representative PET imaging of nanonaps delineating stomach and intestine. BPC, 2,9,16,23-tetra-tert-butyl-29H, 31H-phthalocyanine; ZnBNC, Zinc-2,11,20,29-tetra-tert-butyl-2,3, naphthalocyanine; BNC, 2,11,20,29-tetra-tert-butyl-2,3, naphthalocyanine and ONC, 5,9,14,18,23,27,32,36-octabutoxy-2,3, naphthalocyanine. (Reprinted with permission from Ref 27 Copyright 2014 Nature Publishing Group).

*in vitro*. Presumably, the hydrophobic sensitizers bound to cellular membrane structures such as lysosomes and mitochondria. By contrast, the hydrophilic dyes accumulated inside extranuclear granules and the dyes could be localized during PDT, revealing a granular fluorescence distribution. Similar observations were also obtained from other studies on meso-tetra(4-sulfonatophenyl) porphyrin (TPPS<sub>4</sub>),<sup>33</sup> Nile blue,<sup>34</sup> AlPcS<sub>4</sub> and AlPcS<sub>2</sub>.<sup>35</sup>

### Surfactant-Dispersed Pcs and Ncs for Bioimaging

Surfactants have also been used as Nc or Pc carriers for bioimaging. Silicon 2,3-naphthalocyanine bi

(trihexylsilyloxy) (SiNc) was investigated *in vitro* and *in vivo* for photoacoustic imaging.<sup>36</sup> SiNc was solubilized in 10% Cremophor EL, along with 1% 1,2-propanediol and 1% dimethylformamide in saline by sonication and ICG was used as a control. The Cremophor formulation was shown to have better photostability than ICG. The SiNc Cremophor emulsion was intravenously injected to mice bearing HT 29 tumors. After injection of SiNc, a gradual accumulation of contrast agent in the tumor could be observed with increasing photoacoustic signal (Figure 4).

Recently, a phosphorus Pc dye with its main absorption band beyond 1000 nm was examined for photoacoustic imaging.<sup>37</sup> The dye was dispersed in

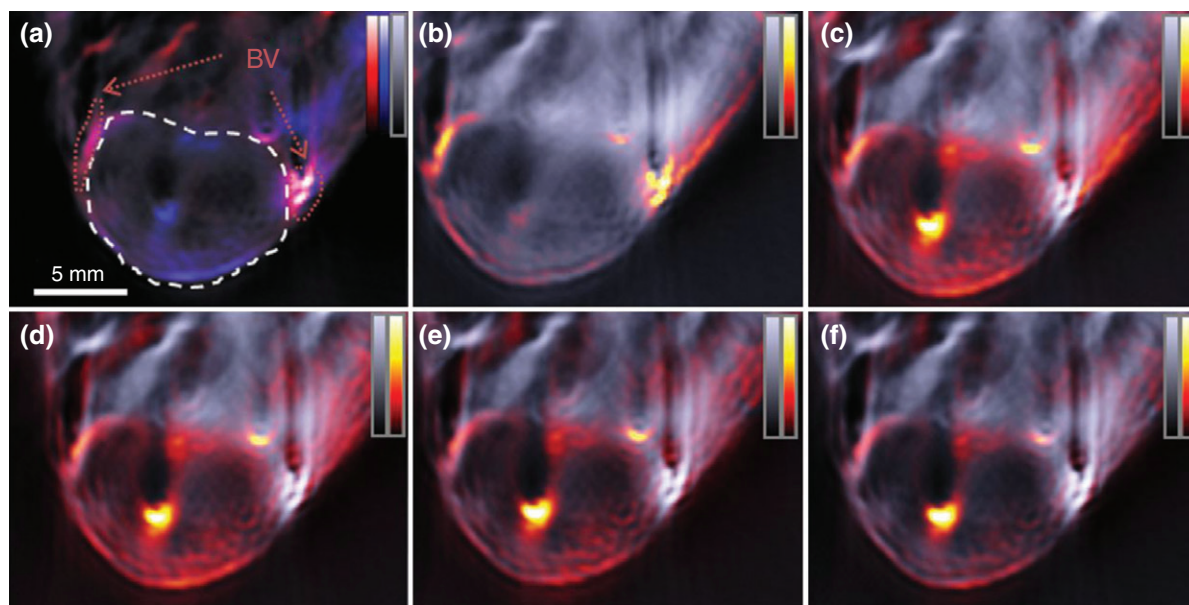


**FIGURE 4** | Photoacoustic images of a mouse bearing a HT29 tumor before and after intravenous injection of SiNc. Greyscale background is overlaid with the signal from SiNc (hot scale). (a) Pre-injection image, indicating tumor (dashed white circle) and surrounding blood vessels (BV, dotted red circles), overlaid with deoxygenated (blue scale) and oxygenated (red scale) hemoglobin signal. (b–f) Images acquired after 5 (B), 15 (C), 30 (D), 45 (E), 60 (F) minutes after intravenous injection of SiNc in a tumor-bearing animal. (Reprinted with permission from Ref 36 Copyright 2015 Society of Nuclear Medicine and Molecular Imaging)

TWEEN surfactant and could be imaged beyond 10 cm in chicken breast phantoms and through a 5 cm arm of a human volunteer. These results underscore the potential of Pcs and Ncs for deep tissue imaging.

### Hydrophilic Modifications of Pcs and Ncs for Bioimaging

Nanoparticle based contrast agents have many merits including accumulation in tumors either by active targeting or by the enhanced permeability and retention effect.<sup>38</sup> However, many water-soluble Pcs or Ncs have been designed and used as contrast agents for imaging as they are more convenient to handle without concerns or limitations of preparation techniques and uniformity control. Water-soluble Pc or Ncs have been synthesized for imaging applications. One study compared different hydrophilic Pcs: phthalocyanine tetrasulfonic acid (PcS4), Zn (II) phthalocyanine tetrasulfonic acid (ZnPcS4), and Al (III) phthalocyanine chloride tetrasulfonic acid (AlPcS4) as contrast agents for photoacoustic images,<sup>39</sup> showing that optical contrast in tumors was greatly enhanced by PcS4 and ZnPcS4 (Figure 5).

Other hydrophilic Pc or Nc conjugates were also designed including saccharide-based conjugates. Hepatic asialoglycoprotein receptors are expressed

on hepatocyte membranes, making lactose and or galactose a putative targeting molecules for liver cancer.<sup>40</sup> Lactose-substituted zinc phthalocyanine, [2,9 (10), 16 (17), 23 (24)-tetrakis ((1-  $\beta$ -D-lactose-2-yl)-1H-1,2,3-triazol-4-yl) methoxyl)phthalocyaninato]zinc(II) was synthesized via click chemistry.<sup>41</sup> After conjugation of lactose, the water solubility and cell specificity were enhanced. Real-time NIR fluorescence imaging was performed with tumor-bearing athymic nude mice after 12 h post tail vein injection. As shown in Figure 6(a), a significant fluorescence increase was detected at the tumor site due to the targeting of lactose-substituted Pc. *Ex vivo* experiments also consistently showed fluorescence was mainly distributed in the liver, tumor, and kidney (Figure 6(b)).

Many MRI contrast agents are gadolinium-based complexes, and large doses are usually required to provide sufficient contrast enhancement.<sup>42</sup> Hydrophilic MRI contrast agents based on Gd or Mn derivatives of tetrapyrroles have been developed.<sup>43</sup> Sulfonated Pcs proved to show good tumor localization although the mechanism of selectivity was not definite, but could be due to the sulfate functional groups,<sup>44</sup> Saini et al. synthesized tetrasodium salt of manganese tetra sulfo phthalocyanine (MnPcS<sub>4</sub>) and used this as a MRI contrast agent in a mouse model of cancer.<sup>43</sup> Molar relaxivity of MnPcS<sub>4</sub> could reach 10.1 (mM)<sup>-1</sup>, two times greater

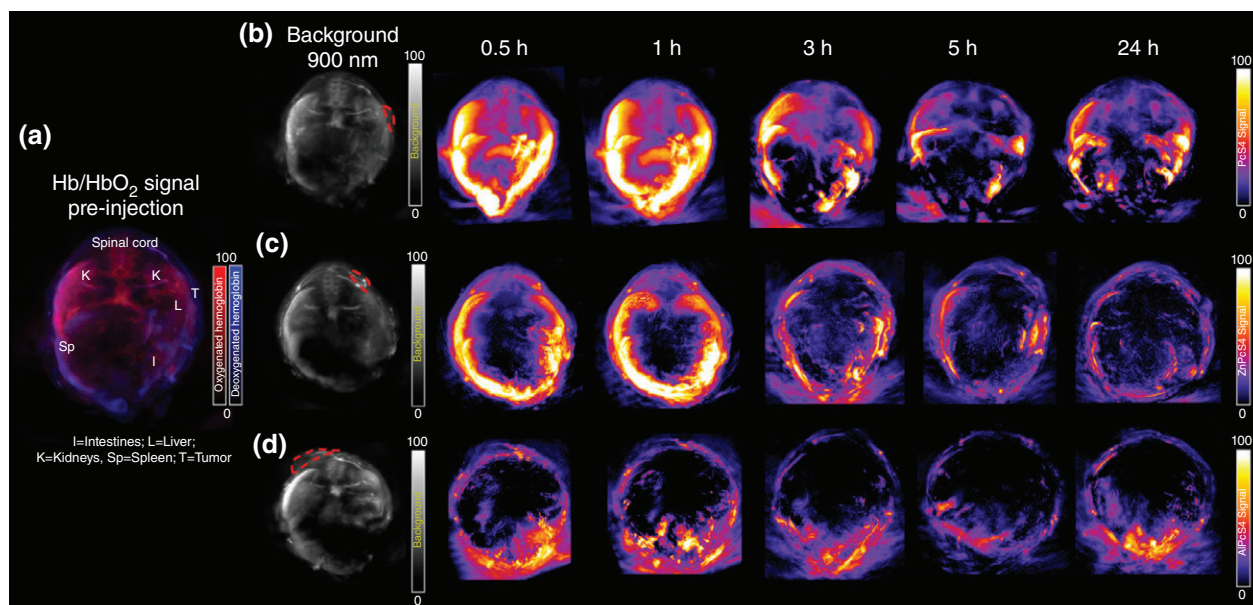


**FIGURE 5** | *In vivo* photoacoustic images showing transverse slices of tumor-bearing mice (a) oxygenated hemoglobin (HbO<sub>2</sub>) and deoxygenated hemoglobin (Hb) signals were acquired before injection of PcS<sub>4</sub>, showing the endogenous contrast between the different organs, the red signal represents HbO<sub>2</sub> while the blue signals represent Hb in the color bar which is normalized within individual deoxygenated and oxygenated hemoglobin signals to give 0–100% scale. Phthalocyanine PA signals at various time points after tail-vein administration of (b) PcS<sub>4</sub> (c) ZnPcS<sub>4</sub> and (d) ALPcS<sub>4</sub>. Background PA signal from the tissues were acquired at 900 nm laser wavelength with the dashed red lines delineating tumor tissue. (Reprinted with permission from Ref 39 Copyright 2015 The Optical Society)

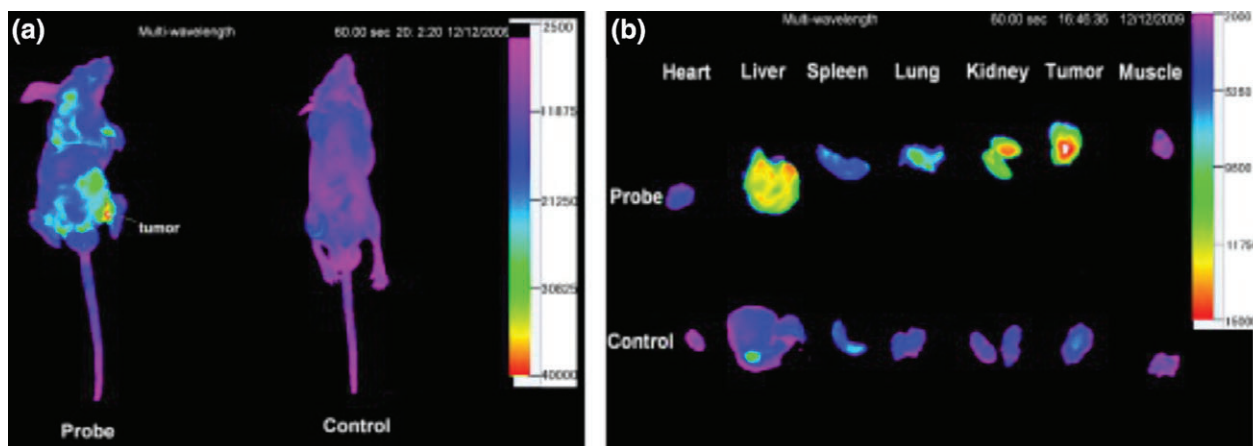


**FIGURE 6** | Optical imaging (a) *in vivo* and (b) fluorescence dissected of dissected organs with lactose substituted Zinc Pc. Liver cancer bearing mice injected with 200  $\mu$ L of  $2 \times 10^{-4}$  mol/L: excitation 625 nm, emission 700 nm. (Reprinted with permission from Ref 41 Copyright 2013 ScienceDirect)

than that of Gd-DTPA. Following intravenous administration of the dye, tumor-to-muscle MnPcS<sub>4</sub> ratio was calculated to be 9.2 :1, demonstrating preferential accumulation of MnPcS<sub>4</sub> in the tumor and MRI contrast enhancement was clearly observed. Also, <sup>64</sup>Cu has been chelated to sulfonated Pcs for PET studies in a tumor-bearing rat model; although one study showed that PET signals was mostly detected from kidneys (20%ID/g) and liver (12%ID/

g) and further work was required to better demark the tumor (0.2% ID/g).<sup>45</sup>

## PHOTOTHERAPY USING Pcs AND Ncs

Pcs and Ncs have been used as photosensitizers for PDT applications. Three fundamental elements of PDT include oxygen, photosensitizers and light

delivery of an appropriate wavelength.<sup>46</sup> Upon irradiation, generated ROS can induce direct toxicity on cells leading to necrosis or apoptosis, result in thrombosis and hemorrhages by vascular damage, further induce acute inflammation with anti-tumor immunity. Generally, the ROS can also cause damage to the plasma membrane, mitochondria, Golgi apparatus, lysosomes, and others.<sup>47</sup> Photochemical internalization is an alternative PDT approach for the specific cytosolic release of molecules such as DNA or toxins, viruses, peptide nucleic acids from endocytic vesicles via the breakdown of the endosomal/lysosomal membranes.<sup>48,49</sup> Besides these, the photothermal effect of Pcs/Ncs has been utilized for cancer hyperthermia, or photothermal therapy (PTT). At elevated temperatures the light-treated location will be damaged by heat, leading to the denaturation of proteins, disruption of the membrane and ablation of tumor. Selective PTT can be achieved by local laser treatment and targeting of Pcs or Ncs to diseased sites.<sup>10</sup> Some composite nanoparticles were also designed for a combination of PDT and PTT.<sup>50</sup> For example, to achieve combined PTT and PDT, nanoparticles are required to have strong absorbance in NIR region and exhibit both photothermal and singlet oxygen conversion efficiency.

Hollow silica nanoparticles (HSNs) were designed made by tetraethoxysilane as a silica source and Pluronic as a template, followed by calcination and removal of template.<sup>51</sup> Then Pc was loaded in HSNs, resulting in composite nanoparticles (Pc@HSNs) that could induce the dual effects of PDT and PTT. As shown in Figure 7, when treated with both Pc@HSNs and laser, the tumors of mice that had S180 murine sarcomas shrank significantly and were eradicated eventually after 5 days with a survival of at least 45 days whereas mice in control group treated with saline, with Pc@HSNs alone or laser alone did not show much anti-tumor effect.

Many Pc- and Nc-based nanoformulations have been developed to solve the hydrophobicity problem including liposomes, polymer conjugates, polymeric micelles, surfactants and others, which will be discussed briefly below.

### Liposomal Pcs and Ncs for Therapy

Liposomes are promising carriers of various cargos including photosensitizers. A liposome formulation for Pc and gold conjugates has been reported.<sup>52</sup> This hybrid conjugate was achieved by thiol tether, then the liposome was prepared with egg yolk lecithin.

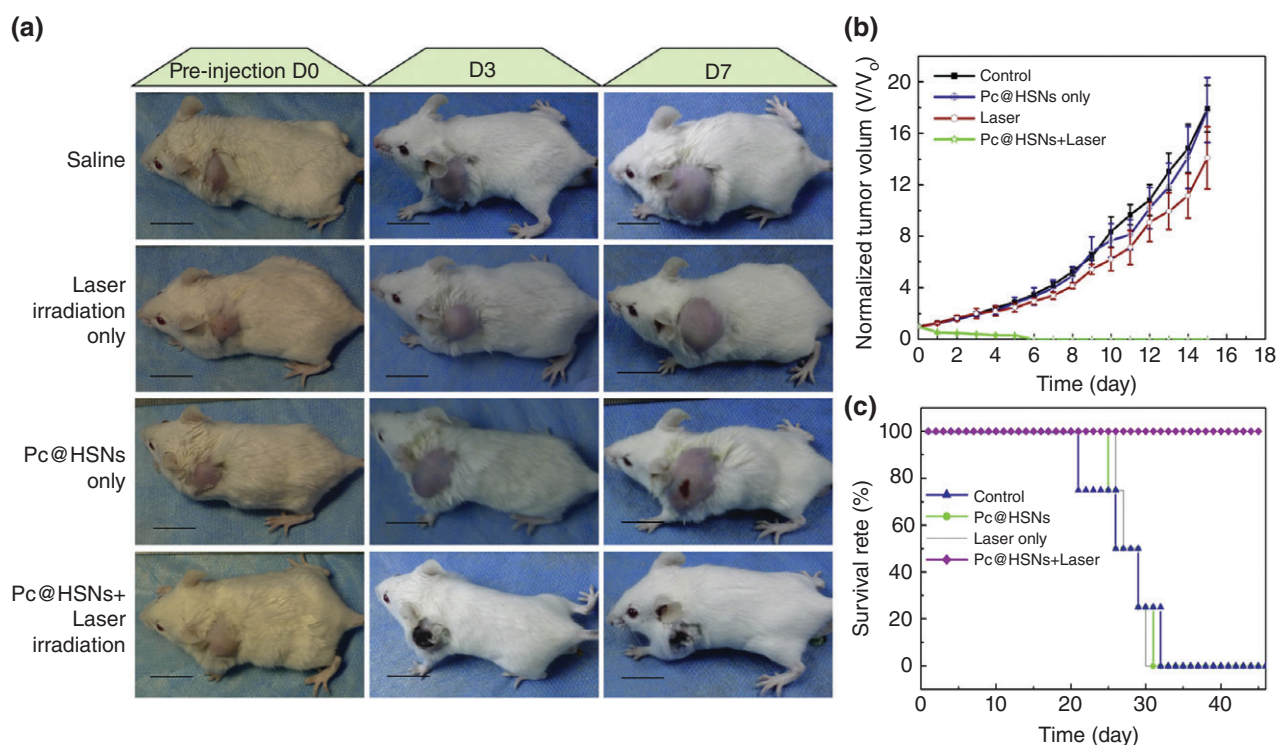


**FIGURE 7** | Phototherapy of Pc encapsulated hollow silica nanoparticles. (a) Representative photos showing tumor treatment outcome of four different groups, treated with saline, laser, Pc@HSNs alone and Pc@HSNs + laser, respectively. Scale bar: 2 cm. (b) Relative tumor volumes of four different groups. (c) Survival curves of four different groups treated as indicated. (Reprinted with permission from Ref 51 Copyright 2013 Elsevier)

The liposome allowed greater uptake and selective accumulation of the photosensitizer in tumor cells, resulting in successful PDT treatment. In addition, liposome formulations are tunable by changing the composition or adding additives such as cholesterol, cardiolipin, glucuronic acid, and PEG.<sup>53</sup> The presence of cholesterol has been found to drastically help stabilize the size of unilamellar liposome from 1000 to about 100 nm,<sup>54</sup> enhancing the stability of the delivery system, and facilitating the photodynamic activation of photosensitizers.<sup>47</sup> Liposomal formulations were incubated with different cell lines at different concentrations. Control cells were incubated with liposomes with neither ZnPc nor light and in a second group cells were incubated with liposomal ZnPc but without cholesterol. In most of these cell lines, no significant toxicity was observed. In contrast, photodynamic activity was observed when different human tumor cell lines were incubated with liposomal ZnPc or free ZnPc that included cholesterol. Liposomal photosensitizers have been reported to have advantages over photosensitizer conjugates.<sup>55</sup> In this study, to improve the selectivity of PDT, monoclonal antibodies and aluminum Pc (AlSPc) were used for the PDT-targeted treatment of human bladder tumor. Two methods were used for targeting; one of them was direct conjugation of antibodies to Pc, and the other was Pc-encapsulated in liposomes conjugated to antibodies. At the same dose of antibody, the liposomal form showed higher phototoxicity by up to 13-fold.

### Pc- and Nc-based Polymeric Nanoparticles and Micelles for Therapy

Biodegradable and biocompatible polymer-based nanotechnology has been used to solubilize hydrophobic Ncs and Pcs. The colloidal carriers including micro/nanospheres, polymer-drug conjugates, and polymeric micelles, are used for delivery of cargos to protect them against degradation, excretion, or side effects. In 1984, Ringsdorf first proposed using polymeric micelles as drug carrier<sup>56</sup> and then polymeric micelles have been emerging as a frequently used carrier systems.<sup>57–60</sup> Leroux et al. studied randomly and terminally alkylated N-isopropylacryl-amide (NIPAM) copolymers loaded with aluminum chloride Pcs (AlClPc). The photosensitizer was loaded by a solvent exchange method; that is, photosensitizer and copolymer were first solubilized in N, N-dimethylformamide and then dialyzed against water for 24 h. PDT treatment was performed and cures were achieved in many of the mice that received a 0.05  $\mu\text{mol/kg}$  dose.<sup>61,62</sup> Poly (lactic-co-glycolic acid) (PLGA), which has been

approved by FDA and used as a suture material for many years has emerged as a common polymer for pharmaceutical use. It was used to encapsulate hydrophobic Zinc Pc by solvent emulsion evaporation method with a yield and encapsulation efficiency of 80 and 70%, respectively.<sup>63</sup> The ZnPc-loaded PLGA nanoparticles were evaluated by incubation with P388-D1 cells for 6 h followed by treatment with red light with a wavelength of 675 nm. After 24 h, 61% cellular death was induced; showing the PDT potential of PLGA-based nanoparticles.

### Pc and Nc Surfactant Formulations for Therapeutic Use

Surfactants are a common delivery vehicle to address the poor solubility of hydrophobic Pcs and Ncs. Among numerous surfactants, Cremophor EL is one of the most common biocompatible surfactants used for the solubilization process. For example, it has been used to solubilize Zn (II)-Pc-disulfide (C11Pc). C11Pc was first conjugated to gold nanoparticles via a thiol tether. A stated advantage of the conjugate was that singlet oxygen does not have to diffuse out of the particles given its structure of encapsulated photosensitizer at the surface.<sup>64</sup> Axially substituted octabutoxy Pc compounds were dissolved in Cremophor by sonication prior to assessment of biodistribution and phototherapeutic efficacy with 740 nm laser excitation.<sup>65</sup> However, ongoing research involves the replacement of organic solvent as well as the Cremophor or Tween with other less toxic solubilizers, considering they might induce negative side effects such as hypersensitivity and neurotoxicity.<sup>66,67</sup>

### Hydrophilic Modifications of Pcs and Ncs for Therapy

Another strategy to improve the solubility of Pc or Nc dyes is to introduce hydrophilic substituents on the periphery of the macrocycle or at the central metal to enable easier solvation.<sup>68</sup> Hydrophilic Pcs can be directly injected into the bloodstream and a number of water soluble tetra- and octa-substituted Pc have been reported. Hydrophilic moieties incorporated on the peripheral macrocycle rings include sulfonates,<sup>69</sup> carboxylates,<sup>70</sup> phosphonates,<sup>71</sup> and quaternarized amino groups.<sup>72</sup> Also, hydrophilic group as axial ligands could be coordinated to the central metal ion of Pcs to improve the solubility.<sup>73,74</sup>

Peripheral and axial substitution of Pc with solketal groups have been compared.<sup>75</sup> The solketal groups substituted Pc dyes in this work were synthesized

from basic chemicals, that is catechol and phthalonitrile. Soketal groups were introduced flexibly before or after the formation of Pc from the basic reactants. It was shown that axially substituted Silicon (Solketal)<sub>8</sub> Pc exhibited less tendency to aggregation and more photocytotoxicity than those of peripherally substituted Zinc (Solketal)<sub>8</sub> Pc, likely due to the prevention of Pc stacking. 2,4, dinitrobenzenesulfonate has been conjugated to zinc Pc.<sup>76</sup> The obtained activatable photosensitizer was demonstrated as a promising fluorescence probe and effective PDT treatment agent. Monoclonal antibodies were conjugated to amino reactive Pc, targeting epidermal growth factor receptors.<sup>77</sup> Conventional photodynamic therapy is based on accumulation of photosensitizers in tumors, but still can lead to damage to normal tissues due to the poor selectivity of photosensitizer. By contrast, photoimmunotherapy is effective when conjugates bind to target cell membranes, improving the specificity. Moreover, the fluorescence of the conjugate can be used to image, monitor, and guide the tumor therapy process. For better solubility and additional functionalities such as improved targeting or enhanced internalization, peptide<sup>78</sup> or amino groups<sup>79</sup> have been also exploited to conjugate Pcs for theranostic application. Arginine-glycine-aspartic acid is a recognition motif of many ligands such as collagen, prothrombin, fibronectin, and vitronectin; Bombesin (BBN) has affinity for gastrin releasing peptide acceptors and a number of tumors overexpress receptors to BBN.<sup>80</sup> These two peptides were recently investigated for targeting Zinc Pc (ZnPc).<sup>78</sup> Particularly, ZnPc-BBN conjugates showed dual roles as both a fluorescence imaging agent and targeting PDT agent.

### Other Formulations for Therapy

Dendrimer phthalocyanine (DPC) has been used as a photosensitizer. With ionic poly (benzyl ether), with a photosensitizer unit in the core, polymer dendrimers could be conjugated in the peripheral forming branching structures. Generally, compared to linear polymers, dendrimers can be modified with rich surface functionalities; the charged surface of dendrimer has interaction with oppositely charged block copolymer via electrostatic interactions, resulting in the formation of supramolecular polyion complex micelle.<sup>81</sup> Dendrimer Ncs have also been developed.<sup>82</sup> Conventional photosensitizers have drawbacks such as aggregation driven by  $\pi$ - $\pi$  stacking or hydrophobic interactions, inhibiting the ROS formation and encapsulation of photosensitizer into nanocarriers. But dendrimer photosensitizers exhibit effective ROS

production, high photocytotoxicity against cancer cells, showing its great potential for PDT. Kataoka et al. developed a novel class of dendrimer Pc (DPC)-loaded poly ethylene glycol-poly L-lysine block copolymer (PEG-PLL) polymeric micelles (DPC/m) with photofrin (polyhematoporphyrin ester, PHE) as a control.<sup>83</sup> DPC/m exhibited 78 folds higher photocytotoxicity than free DPC *in vitro*. Upon light radiation, only DPC/m accumulated in the mitochondria and generated ROS whereas DPC did not show ROS generation in the mitochondria. DPC/m also showed improved antitumor activity *in vivo* compared to PHE even if the dose of DPC/m was 7.3-fold lower than that of PHE. In addition, in the group of PHE treated mice, skin and liver were severely damaged after irradiation of white light, but in the DPC/m-treated group, no such side effects were observed (Figure 8). Also, dendrimer-encapsulated SiNc single agent nanoparticles were developed for both NIR fluorescence imaging and anticancer phototherapy.<sup>82</sup>

Cyclodextrins (CDs), also named cycloamyloses, are a family of cyclic oligosaccharides made up of sugar molecules bound together in a ring. Common natural cyclodextrins include  $\alpha$ -CDs,  $\beta$ -CDs,  $\gamma$ -CDs. These non-toxic molecules can greatly improve the amphiphilicity, biocompatibility, and bioavailability of photosensitizers.<sup>84</sup> Pc-CD conjugates via post modification of PcF<sub>16</sub> by nucleophilic substitution of two fluorine atoms of PcF<sub>16</sub> were made and the photo activities of such conjugates made them great PDT drugs against UM-UC-3 human bladder cancer cells.<sup>85</sup> Another conjugation form is, instead of conjugation on the peripheral of rings of photosensitizer, the conjugation of the dextrin on the axial position.  $\beta$ -CDs were used as axial substituents on silicon (IV) Pcs and it was shown that the conjugates were highly photocytotoxic with IC<sub>50</sub> value of 21 nM, which was about seven-fold lower than similar analogues and tumor treatment efficacy was demonstrated (Figure 9).<sup>86</sup> In order to improve drug loading efficiency, multiple Pc dyes were also encapsulated non-covalently into one dendrimer. Recently, dendrimer-based theranostic agents were designed to encapsulate Pcs dyes and in order to improve the biocompatibility and tumor targeting, with poly (ethylene glycol) (PEG) and luteinizing hormone-releasing hormone (LHRH) conjugated to the nanocarrier.<sup>87</sup> The methyl 4-chloro-4-oxobutyrate (mob) substituted Silica-chelated Pc, PcSi-OH(mob) associated with the nonpolar core of the dendrimer, exhibited NIR absorption at 700 nm and fluorescence emission, which enabled the dual roles of nanoplatfrom, PDT and fluorescence imaging. The LHRH-targeted nanoparticles also showed low

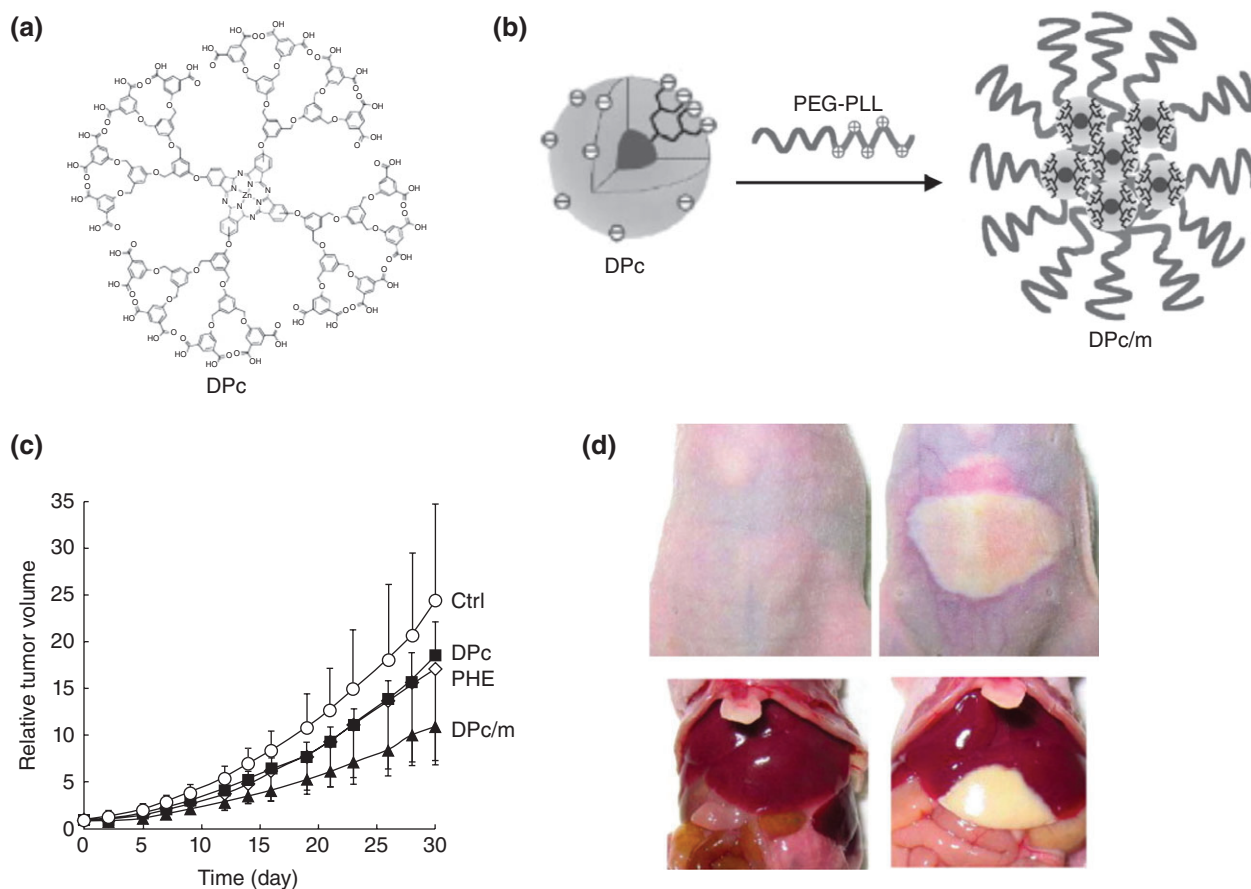


**FIGURE 8** | Tumor treatment using dendrimer Pc encapsulated micelles. (a) Chemical structure of anionic dendrimer phthalocyanine (DPc). (b) DPc encapsulated polyion complex micelle (DPc/m) was formed by mixing DPc and PEG-PLL. (c) Growth curves of subcutaneous A549 tumors in control mice and mice administered with 0.37  $\mu\text{mol/kg}$  DPc, 0.37  $\mu\text{mol/kg}$  DPc/m, and 2.7  $\mu\text{mol/kg}$  PHE ( $n = 6$ ). (d) DPc/m is safe to skin (top left) and liver (bottom left) whereas PHE-induced phototoxicity to skin (top right) and liver (bottom right). 24 hours after administration of photosensitizing agents, the tumors were photoirradiated using a diode laser (fluence: 100  $\text{J}/\text{cm}^2$ ). (Reprinted with permission from Ref 83 Copyright 2009 Elsevier)

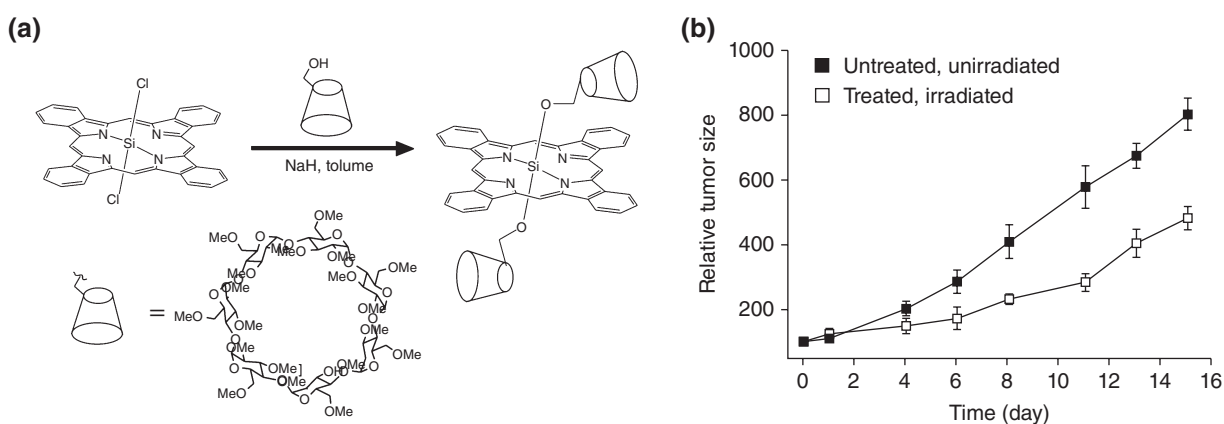


**FIGURE 9** | (a) Schematic illustration of axial conjugation of CD to SiPc, (b) Tumor growth delay after PDT treatment with conjugates. Illumination with laser light (30  $\text{J}/\text{cm}^2$ ) was applied for the PDT. (Reprinted with permission from Ref 86 Copyright 2011 Royal Society of Chemistry)

cytotoxicity with  $\text{IC}_{50}$  value of 28  $\mu\text{g}/\text{mL}$ . As galactose molecules can be recognized by receptors overexpressed in cancer cells, another form of

galactodendritic Pc was also developed as targeting therapeutic agent for PDT treatment of bladder cancer.<sup>88</sup>

Other carriers have also been used to with Pcs and Ncs. Carbon nanotubes have provided some interesting results.<sup>89</sup> Yet, more studies must be done to solve several potential challenges such as biocompatibility of this kind of carbon nanomaterial. In addition, low-density lipoprotein and high-density lipoprotein have been explored as Pc and Nc carriers.<sup>9,90–92</sup>

## CONCLUSIONS

In summary, Pcs and Ncs have unique properties enabling them to be used for biological imaging and therapy. This review highlighted some selected recent developments of Pc- and Nc-based nanoscale formulations that exhibited utility in imaging biological tissues or in phototherapies. Different types of

nanoparticles have been designed to deliver these molecules by targeting approaches or by passive effect. A wide range of chemical substituents can be readily conjugated to the skeleton of Pcs or Ncs peripherally or via central metal chelation.

Although Pcs and Ncs have been used for multiple imaging modalities, their true strength perhaps lies in their stability and high extinction coefficients in the NIR. Therefore, as optical imaging techniques such as PAT gain momentum, there is opportunity for Pcs and Ncs to be used as ideal agents for these techniques. Future challenges include finding unmet clinical needs that can be addressed with NIR optical imaging and phototherapy, and also establishing toxicity profiles. Pcs and Ncs are being increasingly used as new tools in the rapid developing field of theranostics.

## ACKNOWLEDGMENTS

This work was made possible with support from the National Institutes of Health (R01EB017270 and DP5OD017898)

## REFERENCES

1. Josefsen LB, Boyle RW. Unique diagnostic and therapeutic roles of porphyrins and phthalocyanines in photodynamic therapy, imaging and theranostics. *Theranostics* 2012, 2:916–966.
2. Eichhorn H. Mesomorphic phthalocyanines, tetraazaporphyrins, porphyrins and triphenylenes as charge-transporting materials. *J Porphyr Phthalocyanines* 2000, 4:88–102.
3. Zagal JH, Griveau S, Francisco Silva J, Nyokong T, Bedioui F. Metallophthalocyanine-based molecular materials as catalysts for electrochemical reactions. *Coord Chem Rev* 2010, 254:2755–2791.
4. Yourre TA, Rudaya LI, Klimova NV, Shamanin VV. Organic materials for photovoltaic and light-emitting devices. *Semiconductors* 2003, 37:807–815.
5. de la Torre G, Claessens CG, Torres T. Phthalocyanines: old dyes, new materials. Putting color in nanotechnology. *Chem Commun* 2007, 20:2000–2015.
6. Kobayashi N, Furuyama T, Satoh K. Rationally designed phthalocyanines having their main absorption band beyond 1000 nm. *J Am Chem Soc* 2011, 133:19642–19645.
7. D'Souza F, Sandanayaka ASD, Ito O. SWNT-based supramolecular nanoarchitectures with photosensitizing donor and acceptor molecules. *J Phys Chem Lett* 2010, 1:2586–2593.
8. Plaetzer K, Krammer B, Berlanda J, Berr F, Kiesslich T. Photophysics and photochemistry of photodynamic therapy: fundamental aspects. *Lasers Med Sci* 2009, 24:259–268.
9. Mathew S, Murakami T, Nakatsuji H, Okamoto H, Morone N, Heuser JE, Hashida M, Imahori H. Exclusive photothermal heat generation by a gadolinium bis(naphthalocyanine) complex and inclusion into modified high-density lipoprotein nanocarriers for therapeutic applications. *ACS Nano* 2013, 7:8908–8916.
10. Lim C-K, Shin J, Lee Y-D, Kim J, Oh KS, Yuk SH, Jeong SY, Kwon IC, Kim S. Phthalocyanine-aggregated polymeric nanoparticles as tumor-homing near-infrared absorbers for photothermal therapy of cancer. *Theranostics* 2012, 2:871–879.
11. Zhang Y, Song W, Geng J, Chitgupi U, Unsal H, Federizon J, Rzaev J, Sukumaran DK, Alexandridis P, Lovell JF. Therapeutic surfactant-stripped frozen micelles. *Nat Commun* 2016, 7:11649.
12. Jiang Z, Shao J, Yang T, Wang J, Jia L. Pharmaceutical development, composition and quantitative analysis of phthalocyanine as the photosensitizer for cancer photodynamic therapy. *J Pharm Biomed Anal* 2014, 87:98–104.
13. Schreiber I, Hutzler C, Laux P, Berlien H-P, Luch A. Formation of highly toxic hydrogen cyanide upon ruby laser irradiation of the tattoo pigment phthalocyanine blue. *Sci Rep* 2015, 5:12915.
14. Rieffel J, Chitgupi U, Lovell JF. Recent advances in higher-order, multimodal, biomedical imaging agents. *Small* 2015, 11:4445–4461.

15. Xia J, Kim C, Lovell JF. Opportunities for photoacoustic-guided drug delivery. *Curr Drug Targets* 2015, 16:571–581.
16. Kim C, Favazza C, Wang LV. In vivo photoacoustic tomography of chemicals: high-resolution functional and molecular optical imaging at new depths. *Chem Rev* 2010, 110:2756–2782.
17. Taratula O, Patel M, Schumann C, Naleway MA, Pang AJ, He H, Taratula O. Phthalocyanine-loaded graphene nanoplatform for imaging-guided combinatorial phototherapy. *Int J Nanomedicine* 2015, 10:2347–2362.
18. Zhang Y, Lovell JF. Porphyrins as theranostic agents from prehistoric to modern times. *Theranostics* 2012, 2:905–915.
19. Wrenn FR, Good ML, Handler P. The use of positron-emitting radioisotopes for the localization of brain tumors. *Science* 1951, 113:525–527.
20. Ogan MD, Revel D, Brasch RC. Metalloporphyrin contrast enhancement of tumors in magnetic resonance imaging. A study of human carcinoma, lymphoma, and fibrosarcoma in mice. *Invest Radiol* 1987, 22:822–828.
21. Taratula O, Doddapaneni BS, Schumann C, Li X, Bracha S, Milovancev M, Alani AW, Taratula O. Naphthalocyanine-based biodegradable polymeric nanoparticles for image-guided combinatorial phototherapy. *Chem Mater* 2015, 27:6155–6165.
22. Zhao P, Zheng M, Yue C, Luo Z, Gong P, Gao G, Sheng Z, Zheng C, Cai L. Improving drug accumulation and photothermal efficacy in tumor depending on size of ICG loaded lipid-polymer nanoparticles. *Biomaterials* 2014, 35:6037–6046.
23. Zheng X, Xing D, Zhou F, Wu B, Chen WR. Indocyanine green-containing nanostructure as near infrared dual-functional targeting probes for optical imaging and photothermal therapy. *Mol Pharm* 2011, 8:447–456.
24. Li Y, Wen T, Zhao R, Liu X, Ji T, Wang H, Shi X, Shi J, Wei J, Zhao Y, et al. Localized electric field of plasmonic nanoplatform enhanced photodynamic tumor therapy. *ACS Nano* 2014, 8:11529–11542.
25. Geng J, Zhu Z, Qin W, Ma L, Hu Y, Gurzadyan GG, Tang BZ, Liu B. Near-infrared fluorescence amplified organic nanoparticles with aggregation-induced emission characteristics for in vivo imaging. *Nanoscale* 2014, 6:939–945.
26. Xiong L, Cao F, Cao X, Guo Y, Zhang Y, Cai X. Long-term-stable near-infrared polymer dots with ultrasmall size and narrow-band emission for imaging tumor vasculature in vivo. *Bioconjug Chem* 2015, 26:817–821.
27. Zhang Y, Jeon M, Rich LJ, Hong H, Geng J, Zhang Y, Shi S, Barnhart TE, Alexandridis P, Huizinga JD, et al. Non-invasive multimodal functional imaging of the intestine with frozen micellar naphthalocyanines. *Nat Nanotechnol* 2014, 9:631–638.
28. Lee C, Kim J, Zhang Y, Jeon M, Liu C, Song L, Lovell JF, Kim C. Dual-color photoacoustic lymph node imaging using nanoformulated naphthalocyanines. *Biomaterials* 2015, 73:142–148.
29. Goldstein JL, Anderson RG, Brown MS. Coated pits, coated vesicles, and receptor-mediated endocytosis. *Nature* 1979, 279:679–685.
30. Reddi E, Castro GL, Biolo R, Jori G. Pharmacokinetic studies with zinc (II)-phthalocyanine in tumour-bearing mice. *Br J Cancer* 1987, 56:597.
31. van Leengoed HL, Cuomo V, Versteeg AA, Van der Veen N, Jori G, Star WM. In vivo fluorescence and photodynamic activity of zinc phthalocyanine administered in liposomes. *Br J Cancer* 1994, 69:840.
32. Steiner R. Dynamic fluorescence changes during photodynamic therapy in vivo and in vitro of hydrophilic Al (III) phthalocyanine tetrasulphonate and lipophilic Zn (II) phthalocyanine administered in liposomes. *J Photochem Photobiol B* 1996, 36:127–133.
33. Berg K, Madslie K, Bommer JC, Oftebro R, Winkelman JW, Moan J. Light induced relocalization of sulfonated meso-tetraphenylporphines in nhik 3025 cells and effects of dose fractionation. *Photochem Photobiol* 1991, 53:203–210.
34. Lin C-W, Shulok JR, Kirley SD, Bachelder CM, Flotte TJ, Sherwood ME, Cincotta L, Foley JW. Photodynamic destruction of lysosomes mediated by Nile blue photosensitizers. *Photochem Photobiol* 1993, 58:81–91.
35. Peng Q, Farrants GW, Madslie K, Bommer JC, Moan J, Danielsen HE, Nesland JM. Subcellular localization, redistribution and photobleaching of sulfonated aluminum phthalocyanines in a human melanoma cell line. *Int J Cancer* 1991, 49:290–295.
36. Bézière N, Ntziachristos V. Optoacoustic Imaging of naphthalocyanine: potential for contrast enhancement and therapy monitoring. *J Nucl Med* 2015, 56:323–328.
37. Zhou Y, Wang D, Zhang Y, Chitgupi U, Geng J, Wang Y, Zhang Y, Cook TR, Xia J, Lovell JF. A phosphorus phthalocyanine formulation with intense absorbance at 1000 nm for deep optical imaging. *Theranostics* 2016, 6:688–697.
38. Luo D, Carter KA, Lovell JF. Nanomedical engineering: shaping future nanomedicines. *WIREs Nanomed Nanobiotechnol* 2015, 7:169–188.
39. Attia ABE, Balasundaram G, Driessen W, Ntziachristos V, Olivo M. Phthalocyanine photosensitizers as contrast agents for in vivo photoacoustic tumor imaging. *Biomed Opt Express* 2015, 6:591–598.
40. Ma P, Liu S, Huang Y, Chen X, Zhang L, Jing X. Lactose mediated liver-targeting effect observed by ex vivo imaging technology. *Biomaterials* 2010, 31:2646–2654.

41. Lv F, He X, Wu L, Liu T. Lactose substituted zinc phthalocyanine: a near infrared fluorescence imaging probe for liver cancer targeting. *Bioorg Med Chem Lett* 2013, 23:1878–1882.
42. Meerovich IG, Gulyaev MV, Meerovich GA, Belov MS, Derkacheva VM, Dolotova OV, Loschenov VB, Baryshnikov AY, Pirogov YA. Study of phthalocyanine derivatives as contrast agents for magnetic resonance imaging. *Russ J Gen Chem* 2015, 85:333–337.
43. Saini SK, Jena A, Dey J, Sharma AK, Singh R. MnPcS 4: a new MRI contrast enhancing agent for tumor localisation in mice. *Magn Reson Imaging* 1995, 13:985–990.
44. Chan W-S, Marshall JF, Svensen R, Bedwell J, Hart IR. Effect of sulfonation on the cell and tissue distribution of the photosensitizer aluminum phthalocyanine. *Cancer Res* 1990, 50:4533–4538.
45. Soucy-Faulkner A, Rousseau JA, Langlois R, Berard V, Lecomte R, Benard F, van Lier JE. Copper-64 labeled sulfophthalocyanines for positron emission tomography (PET) imaging in tumor-bearing rats. *J Porphyr Phthalocyanines* 2008, 12:49–53.
46. Lovell JF, Liu TWB, Chen J, Zheng G. Activatable photosensitizers for imaging and therapy. *Chem Rev* 2010, 110:2839–2857.
47. De Oliveira CA, Kohn LK, Antonio MA, Carvalho JE, Moreira MR, Machado AE, Pessine FB. Photoinactivation of different human tumor cell lines and sheep red blood cells in vitro by liposome-bound Zn (II) Phthalocyanine: effects of cholesterol. *J Photochem Photobiol B* 2010, 100:92–99.
48. Selbo PK, Weyergang A, Høgset A, Norum O-J, Berstad MB, Vikdal M, Berg K. Photochemical internalization provides time-and space-controlled endolysosomal escape of therapeutic molecules. *J Control Release* 2010, 148:2–12.
49. Lu H-L, Syu W-J, Nishiyama N, Kataoka K, Lai P-S. Dendrimer phthalocyanine-encapsulated polymeric micelle-mediated photochemical internalization extends the efficacy of photodynamic therapy and overcomes drug-resistance in vivo. *J Control Release* 2011, 155:458–464.
50. Bhana S, O'Connor R, Johnson J, Ziebarth JD, Henderson L, Huang X. Photosensitizer-loaded gold nanorods for near infrared photodynamic and photothermal cancer therapy. *J Colloid Interface Sci* 2016, 469:8–16.
51. Peng J, Zhao L, Zhu X, Sun Y, Feng W, Gao Y, Wang L, Li F. Hollow silica nanoparticles loaded with hydrophobic phthalocyanine for near-infrared photodynamic and photothermal combination therapy. *Biomaterials* 2013, 34:7905–7912.
52. Nombona N, Maduray K, Antunes E, Karsten A, Nyokong T. Synthesis of phthalocyanine conjugates with gold nanoparticles and liposomes for photodynamic therapy. *J Photochem Photobiol B* 2012, 107:35–44.
53. Nunes SMT, Sguilla FS, Tedesco AC. Photophysical studies of zinc phthalocyanine and chloroaluminum phthalocyanine incorporated into liposomes in the presence of additives. *Braz J Med Biol Res* 2004, 37:273–284.
54. Oliveira CA, Machado AEH, Pessine FBT. Preparation of 100 nm diameter unilamellar vesicles containing zinc phthalocyanine and cholesterol for use in photodynamic therapy. *Chem Phys Lipids* 2005, 133:69–78.
55. Morgan J, Lottman H, Abbou CC, Chopin DK. Comparison of direct and liposomal antibody conjugates of sulfonated aluminum phthalocyanines for selective photoimmunotherapy of human bladder-carcinoma. *Photochem Photobiol* 1994, 60:486–496.
56. Bader H, Ringsdorf H, Schmidt B. Watersoluble polymers in medicine. *Die Angew Makromol Chem* 1984, 123:457–485.
57. van Nostrum CF. Polymeric micelles to deliver photosensitizers for photodynamic therapy. *Adv Drug Deliv Rev* 2004, 56:9–16.
58. Kwon GS, Okano T. Polymeric micelles as new drug carriers. *Adv Drug Deliv Rev* 1996, 21:107–116.
59. Allen C, Maysinger D, Eisenberg A. Nano-engineering block copolymer aggregates for drug delivery. *Colloids Surf B Biointerfaces* 1999, 16:3–27.
60. Kataoka K, Harada A, Nagasaki Y. Block copolymer micelles for drug delivery: design, characterization and biological significance. *Adv Drug Deliv Rev* 2001, 47:113–131.
61. Taillefer J, Jones M-C, Brasseur N, Van Lier JE, Leroux J-C. Preparation and characterization of pH-responsive polymeric micelles for the delivery of photosensitizing anticancer drugs. *J Pharm Sci* 2000, 89:52–62.
62. Le Garrec D, Taillefer J, Van Lier JE, Lenaerts V, Leroux J-C. Optimizing pH-responsive polymeric micelles for drug delivery in a cancer photodynamic therapy model. *J Drug Target* 2002, 10:429–437.
63. Ricci-Júnior E, Marchetti JM. Zinc(II) phthalocyanine loaded PLGA nanoparticles for photodynamic therapy use. *Int J Pharm* 2006, 310:187–195.
64. Camerin M, Magaraggia M, Soncin M, Jori G, Moreno M, Chambrier I, Cook MJ, Russell DA. The in vivo efficacy of phthalocyanine-nanoparticle conjugates for the photodynamic therapy of amelanotic melanoma. *Eur J Cancer* 2010, 46:1910–1918.
65. Soncin M, Busetti A, Reddi E, Jori G, Rither BD, Kenney ME, Rodgers MA. Pharmacokinetic and phototherapeutic properties of axially substituted Si (IV)-tetradibenzobarreleno-octabutoxyphthalocyanines. *J Photochem Photobiol B* 1997, 40:163–167.
66. ten Tije AJ, Verweij J, Loos WJ, Sparreboom A. Pharmacological effects of formulation vehicles: implications for cancer chemotherapy. *Clin Pharmacokinet* 2003, 42:665–685.

67. Gelderblom H, Verweij J, Nooter K, Sparreboom A. Cremophor EL: the drawbacks and advantages of vehicle selection for drug formulation. *Eur J Cancer* 2001, 37:1590–1598.
68. Tedesco AC, Rotta JC, Lunardi CN. Synthesis, photophysical and photochemical aspects of phthalocyanines for photodynamic therapy. *Curr Org Chem* 2003, 7:187–196.
69. Ogunsipe A, Nyokong T. Photophysical and photochemical studies of sulphonated non-transition metal phthalocyanines in aqueous and non-aqueous media. *J Photochem Photobiol Chem* 2005, 173:211–220.
70. Kahl SB, Li J. Synthesis and characterization of a boronated metallophthalocyanine for boron neutron capture therapy. *Inorg Chem* 1996, 35:3878–3880.
71. Sharman WM, Kudrevich SV, van Lier JE. Novel water-soluble phthalocyanines substituted with phosphonate moieties on the benzo rings. *Tetrahedron Lett* 1996, 37:5831–5834.
72. De Filippis MP, Dei D, Fantetti L, Roncucci G. Synthesis of a new water-soluble octa-cationic phthalocyanine derivative for PDT. *Tetrahedron Lett* 2000, 41:9143–9147.
73. Durmus M, Nyokong T. The synthesis, fluorescence behaviour and singlet oxygen studies of new water-soluble cationic gallium (III) phthalocyanines. *Inorg Chem Commun* 2007, 10:332–338.
74. Zhu Y-J, Huang J-D, Jiang X-J, Sun J-C. Novel silicon phthalocyanines axially modified by morpholine: synthesis, complexation with serum protein and in vitro photodynamic activity. *Inorg Chem Commun* 2006, 9:473–477.
75. Hofman J-W, van Zeeland F, Turker S, Talsma H, Lambrechts SAG, Sakharov DV, Hennink WE, van Nostrum CF. Peripheral and axial substitution of phthalocyanines with solketal groups: synthesis and in vitro evaluation for photodynamic therapy. *J Med Chem* 2007, 50:1485–1494.
76. He H, Lo P-C, Ng DKP. A glutathione-activated phthalocyanine-based photosensitizer for photodynamic therapy. *Chemistry* 2014, 20:6241–6245.
77. Mitsunaga M, Ogawa M, Kosaka N, Rosenblum LT, Choyke PL, Kobayashi H. Cancer cell-selective in vivo near infrared photoimmunotherapy targeting specific membrane molecules. *Nat Med* 2011, 17:1685–1691.
78. Ranyuk E, Cauchon N, Klarskov K, Guérin B, van Lier JE. Phthalocyanine-peptide conjugates: receptor-targeting bifunctional agents for imaging and photodynamic therapy. *J Med Chem* 2013, 56:1520–1534.
79. Chen Z, Xu P, Chen J, Chen H, Hu P, Chen X, Lin L, Huang Y, Zheng K, Zhou S, et al. Zinc phthalocyanine conjugated with the amino-terminal fragment of urokinase for tumor-targeting photodynamic therapy. *Acta Biomater* 2014, 10:4257–4268.
80. Xiao D, Wang J, Hampton LL, Weber HC. The human gastrin-releasing peptide receptor gene structure, its tissue expression and promoter. *Gene* 2001, 264:95–103.
81. Jang W-D, Nishiyama N, Kataoka K. Supramolecular assembly of photofunctional dendrimers for biomedical nano-devices. *Supramol Chem* 2007, 19:309–314.
82. Taratula O, Schumann C, Duong T, Taylor KL, Taratula O. Dendrimer-encapsulated naphthalocyanine as a single agent-based theranostic nanopatform for near-infrared fluorescence imaging and combinatorial anticancer phototherapy. *Nanoscale* 2015, 7:3888–3902.
83. Nishiyama N, Nakagishi Y, Morimoto Y, Lai P-S, Miyazaki K, Urano K, Horie S, Kumagai M, Fukushima S, Cheng Y, et al. Enhanced photodynamic cancer treatment by supramolecular nanocarriers charged with dendrimer phthalocyanine. *J Control Release* 2009, 133:245–251.
84. Sortino S, Mazzaglia A, Monsù Scolaro L, Marino Merlo F, Valveri V, Sciortino MT. Nanoparticles of cationic amphiphilic cyclodextrins entangling anionic porphyrins as carrier-sensitizer system in photodynamic cancer therapy. *Biomaterials* 2006, 27:4256–4265.
85. Lourenço LMO, Pereira PMR, Maciel E, Válega M, Domingues FMJ, Domingues MRM, Neves MGPMS, Cavaleiro JAS, Fernandes R, Tomé JPC. Amphiphilic phthalocyanine-cyclodextrin conjugates for cancer photodynamic therapy. *Chem Commun* 2014, 50:8363.
86. Lau JTF, Lo P-C, Tsang Y-M, Fong W-P, Ng DKP. Unsymmetrical  $\beta$ -cyclodextrin-conjugated silicon(iv) phthalocyanines as highly potent photosensitizers for photodynamic therapy. *Chem Commun* 2011, 47:9657.
87. Taratula O, Schumann C, Naleway MA, Pang AJ, Chon KJ, Taratula O. A multifunctional theranostic platform based on phthalocyanine-loaded dendrimer for image-guided drug delivery and photodynamic therapy. *Mol Pharm* 2013, 10:3946–3958.
88. Pereira PMR, Silva S, Cavaleiro JAS, Ribeiro CAF, Tomé JPC, Fernandes R. Galactodendritic phthalocyanine targets carbohydrate-binding proteins enhancing photodynamic therapy. *PLoS One* 2014, 9:e95529.
89. Menon JU, Jadeja P, Tambe P, Vu K, Yuan B, Nguyen KT. Nanomaterials for photo-based diagnostic and therapeutic applications. *Theranostics* 2013, 3:152–166.
90. Li H, Marotta DE, Kim S, Busch TM, Wileyto EP, Zheng G. High payload delivery of optical imaging and photodynamic therapy agents to tumors using phthalocyanine-reconstituted low-density lipoprotein nanoparticles. *J Biomed Opt* 2005, 10:41203.
91. Song L, Li H, Sunar U, Chen J, Corbin I, Yodh AG, Zheng G. Naphthalocyanine-reconstituted LDL nanoparticles for in vivo cancer imaging and treatment. *Int J Nanomedicine* 2007, 2:767–774.
92. Ng KK, Lovell JF, Zheng G. Lipoprotein-inspired nanoparticles for cancer theranostics. *Acc Chem Res* 2011, 44:1105–1113.